



CERN-ACC-NOTE-2023-0004

2023-02-27

Charlotte.Duchemin@cern.ch

Thierry.Stora@cern.ch

Isotope production induced by 1.4 GeV PS Booster: reaction channels identified from secondary particle fields in thick targets

*Charlotte Duchemin, Francesco Cerutti, Sebastian Rothe, Francesc Salvat Pujol, Thierry Stora,
Joachim Vollaire*

Organisation Européenne pour la Recherche Nucléaire (CERN), Geneva, Switzerland
Institute for Nuclear and Radiation Physics, IKS, KU Leuven, Leuven, Belgium

Keywords: ISOLDE, FLUKA, PSB, alpha, tritium, secondary particles, reactions, TENDL-2019, Hg-208

Abstract

This note describes systematic investigations of isotope production channels in thick targets exposed to the PS Booster (PSB) beam at ISOLDE. Recent experimental results have shown that new important radionuclide beams could be produced such as Pb-nat(p,x)Hg-208 in thick lead targets. We introduce in this note calculations of the production yield of isotopes generated from the creation and re-interaction of α particles in thick lead, bismuth, thorium and uranium targets irradiated by the 1.4 GeV proton beam delivered from the CERN PS Booster at ISOLDE. It gives the production yields of several isotopes that are not directly predicted with FLUKA and its RESNUCLEI production card while keeping a reasonable CPU time. These isotopes are particularly produced from (α , xp) and (^3H , yp) reactions, with $x = 4, 5, 6$ and $y = 3, 4, 5$. The production yields have been calculated for Pb-208, Bi-209, Th-232 and U-238 target nuclei. The TENDL-2019 library has been used to recover the production cross-sections together with the afore-mentioned version of FLUKA to score the α and ^3H fluences. The calculation method was verified with the FLUKA predictions for the Bi-209(α ,2n) reaction and the At-211 production yield, an isotope of high interest in nuclear medicine, as well as with the radionuclides which are produced via (^3H ,3p) and (α ,2p) reactions. The computation and experimental data are in good agreement, providing an alternative method to evaluate the inventories of radionuclides of potential interest for target waste management, and for the physics and medical programs at ISOLDE and MEDICIS.

This is an internal CERN publication and does not necessarily reflect the views of the CERN management.

CERN-ACC-NOTE-2023-0004
10/02/2023



Contents

1	Introduction	1
2	Methodology applied to the calculation of the Hg-208 yield.....	1
3	Results	4
4	Validation of the approach and with experimental data.....	5
5	Impact of a 2 GeV proton beam energy on these reaction channels	7
6	Conclusions	7
7	References	7

1 Introduction

This work is motivated by the detection of Hg-208 beams (β^- emitter, $T_{1/2} = 41$ min) produced at ISOLDE during the irradiation of a thick lead target with the 1.4 GeV proton beam delivered by the PS Booster in 2014 and 2016, for which the results have been recently published [1]. This radionuclide can be produced by $(\alpha,4p)$ and $(^3\text{H},3p)$ reactions on Pb-208 (52.4% in Pb-nat). The α and ^3H particles are produced as secondary particles from the interaction of the proton beam with the thick lead target. However, the FLUKA code [2, 3, 4] does not predict the production of Hg-208 in lead since this isotope has a too low production rate to be estimated with a Monte Carlo code with reasonable CPU time. The production of nuclei through secondary particle re-interaction (such as ^2H , ^3H , ^3He and α particles) was included in FLUKA test version 2006.3 and triggered by the experimental identification of Bi-209(p,x)At-211 and Pb-nat(p,x)At-211 new reaction channels at ISOLDE [5]. However, such production yields cannot be computed presently even with a very high number of primary particles and high statistics. This note proposes an alternative method to calculate the production yield of radionuclides produced by the re-interaction of secondary particles¹. The CERN FLUKA code version 4.1 has been used to generate the results presented in the following sections².

2 Methodology applied to the calculation of the Hg-208 yield

It is possible to produce Hg-208 from two nuclear reactions on Pb-208, the most abundant lead stable isotope (52.4%) [7]. Possible reaction channels were previously reported as possible mechanisms such as photonuclear reactions, double-neutron captures, the re-interaction of secondary pions and the implication of secondary reactions induced by ^3He and ^4He . Reaction channels such as (p,π^-xn) , $(^3\text{He},xn)$, $(^4\text{He},xn)$ were already considered for the production of Po-210 and At-211 from LBE (liquid Lead Bismuth Eutectic) targets, the latter two reactions being only considered for the production of radionuclides located in the east part of the nuclide chart with respect to the target nucleus (see Fig.1).

Po 210 138.376 d α 5.30433... γ (603) α <0.0005 + <0.030 α 0.002 $\sigma_{\text{th}} < 0.1$	Po 211 25.2 s 516 ms α 7.275 α 11.45... α 7.450... 1064...IT γ (898) γ (363...) 570... 583 IT 10.22 8.785	Po 212 45.1 s 17.1 ns 0.3 μs α 6.6229 α 11.65... α 7.450... 1064...IT γ (898) γ (363...) 570... 583 IT 10.22 8.785	At 211 7.214 h α 5.8695... γ (687...)	At 212 119 ms 314 ms α 7.84 α 7.90... α 7.62... α 7.63... α 9.079	At 213 125 ns	Pu 240 6561 a α 5.168 α 5.124... α (45...), e^- , g α 290 $\sigma_{\text{th}} < 0.059$	Pu 241 14329 a β^- 0.02, g α 4.896... γ (149...) σ 370, σ 1010	Pu 242 3.73 $\cdot 10^4$ a β^- 4.902, 4.858... γ (45...), e^- , g α (149...) σ 18, σ < 0.2
Bi 209 100 2.01 $\cdot 10^{19}$ a α 3.077... α 0.011 + 0.023 $\sigma_{\text{th}} < 3E-7$	Bi 210 3.04 $\cdot 10^4$ a 5.012 d α 4.946 α 4.959... α 4.656 α 2.66 α 305 α 0.054 $\sigma_{\text{th}} < 3E-6$	Bi 211 2.14 m α 6.6229 α 11.65... α 7.450... 1064...IT γ (898) γ (363...) 570... 583 IT 10.22 8.785	Po 210 138.376 d α 5.30433... γ (603) α <0.0005 + <0.030 α 0.002 $\sigma_{\text{th}} < 0.1$	Po 211 25.2 s 516 ms α 7.275 α 11.45... α 7.450... 1064...IT γ (898) γ (363...) 570... 583 IT 10.22 8.785	Po 212 45.1 s 17.1 ns 0.3 μs α 6.6229 α 11.65... α 7.450... 1064...IT γ (898) γ (363...) 570... 583 IT 10.22 8.785	Np 239 2.356 d β^- 0.4, 0.7... γ 106, 278 228... e^- , g σ 32 + 19, σ < 1	Np 240 7.22 m 61.9 m β^- 2.2... α 556, 597... α 566, 574 α 601, 448... α 19	Np 241 13.9 m β^- 1.3... γ 175, (133...) e^- , g
Pb 208 52.4 σ 0.00023 $\sigma_{\text{th}} < 8E-6$	Pb 209 3.234 h β^- 0.644 σ < 0.5	Pb 210 22.20 a β^- 0.02, 0.06 γ 47, e^- , g α 3.72 σ < 0.5	Bi 209 100 2.01 $\cdot 10^{19}$ a α 3.077... α 0.011 + 0.023 $\sigma_{\text{th}} < 3E-7$	Bi 210 3.04 $\cdot 10^4$ a 5.012 d α 4.946 α 4.959... α 4.656 α 2.66 α 305 α 0.054 $\sigma_{\text{th}} < 3E-6$	Bi 211 2.14 m α 6.6229 α 11.65... α 7.450... 1064...IT γ (898) γ (363...) 570... 583 IT 10.22 8.785	U 238 99.2742 280 ns α 4.468 $\cdot 10^4$ a IT 2513 γ (50...), e^- 1879... α , σ 27 σ < 0.6	U 239 23.45 m β^- 1.2, 1.3... γ 75, 44... e^- σ 22, σ 15	U 240 14.1 h β^- 0.360... γ 44, (190...) e^- , g
Tl 207 1.33 s 4.77 m IT 997 β^- 1.4... γ 351 γ (898...)	Tl 208 3.053 m β^- 1.8, 2.4... γ 2615, 583 511, 860, 277... 117...	Tl 209 2.162 m β^- 1.8... γ 1567, 465 117...	Pb 208 52.4 σ 0.00023 $\sigma_{\text{th}} < 8E-6$	Pb 209 3.234 h β^- 0.644 σ < 0.5	Pb 210 22.20 a β^- 0.02, 0.06 γ 47, e^- , g α 3.72 σ < 0.5	Pa 237 8.7 m β^- 1.4, 2.3... γ 854, 865 529 541...	Pa 238 2.28 m β^- 1.7, 2.9... γ 1015, 635 446, 680... g	Pa 239 1.8 h β^- 522, 562, 638 681
Hg 206 8.15 m β^- 1.5... γ 305, 650... g	Hg 207 2.9 m β^- 1.8... γ 351, 997 1637... β^-	Hg 208 ~42 m β^- 1.8... γ 474	Tl 207 1.33 s 4.77 m IT 997 β^- 1.4... γ 351 γ (898...)	Tl 208 3.053 m β^- 1.8, 2.4... γ 2615, 583 511, 860, 277... 117...	Tl 209 2.162 m β^- 1.8... γ 1567, 465 117...	Th 236 37.5 m β^- 1.0... γ 111, (647 196...)	Th 237 5.0 m β^-	Th 238 9.4 m β^- 89

¹ A preliminary study on the Hg-208 yield calculation was performed in 2014 [6]

² At the time of the publication of this note (February 2023) the current released version is 4.3. While several important improvements of different physics processes have been included since version 4.1, none of them impact the α and ^3H fluences shown in Fig. 3 beyond the depicted statistical uncertainties.

Fig. 1: Region of interest for different heavy target materials such as Pb, Bi, and U, populating radionuclides of interest for physics, medical or waste handling aspects such as Po-210, Hg-208, At-211, Pa-239.

Figure 2 shows the production cross-section of Hg-208 from Pb-208($^3\text{H},3\text{p}$) and Pb-208($\alpha,4\text{p}$) reactions, given by the TENDL-2019 library that is based on the output of the TALYS nuclear model code [8]. Both cross-sections show a decreasing tendency at 200 MeV. The Q-value of the Pb-208($^3\text{H},3\text{p}$) reaction is -15.40 MeV and the Q-value of the Pb-208($\alpha,4\text{p}$) reaction is -35.21 MeV.

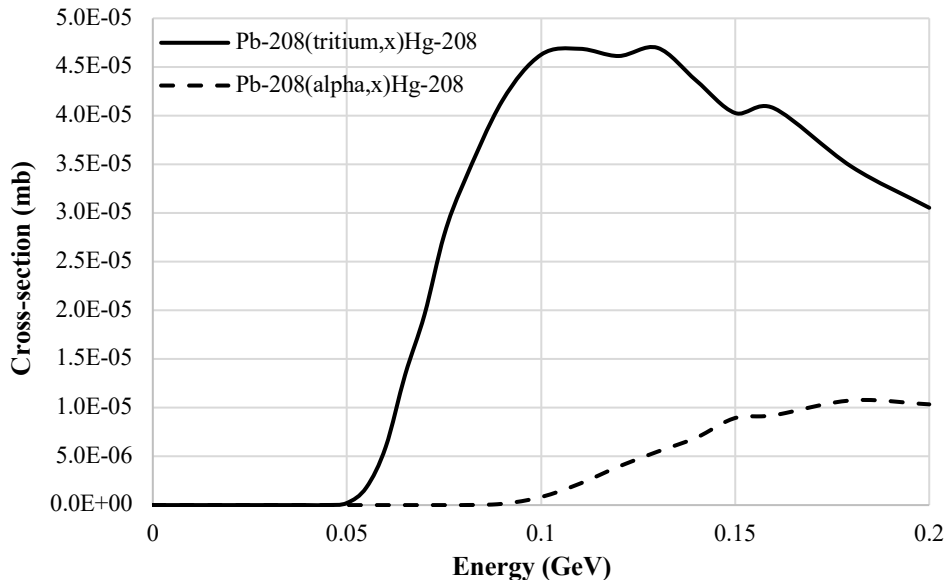


Fig. 2: Hg-208 production cross-sections from ^3H and α interaction with Pb-208 extracted from TENDL-2019

In the absence of the possibility of directly evaluating the Hg-208 yield with FLUKA, an alternative approach is to calculate the ^3H and α particle fluences resulting from the interaction of the 1.4 GeV proton beam impinging on a lead ISOLDE target (cylinder, $r = 0.7$ cm, $L = 19.6$ cm, $V = 30.2$ cm 3 , $\rho = 10.7$ g.cm $^{-3}$) and subsequent convolution with the cross-section data depicted in Figure 2. This is performed by scoring the ^3H and α particle track-lengths inside the entire lead target volume with the USRTRACK card of FLUKA. This is performed by scoring the ^3H and α particle track-lengths in a discrete energy bin structure, with bins ranging from 0.1 MeV to the primary beam energy using 320 logarithmic spaced intervals for sufficient binning. Providing the respective region volume for normalization this detector eventually yields the differential distribution of the fluences in cm $^{-2}$.GeV $^{-1}$.primary $^{-1}$. By integrating the differential distribution of the fluences $d\Phi/dE$ over the respective energy bins (dE), one gets the total fluences per bin in cm $^{-2}$.primary $^{-1}$ (see Figure 3). The energy range for which both fluences and cross-section data are available is shaded in blue in Figure 3. This range represents 28% of the total ^3H fluence and 35% of the total α fluence. One has also to consider that 43% of the total ^3H fluence is below the energy threshold of the Pb-208($^3\text{H},3\text{p}$) reaction. Also, 54% of the total α fluence is below the energy threshold of the Pb-208($\alpha,4\text{p}$) reaction. Therefore, in both cases, half of the total fluence does not contribute to the production of Hg-208.

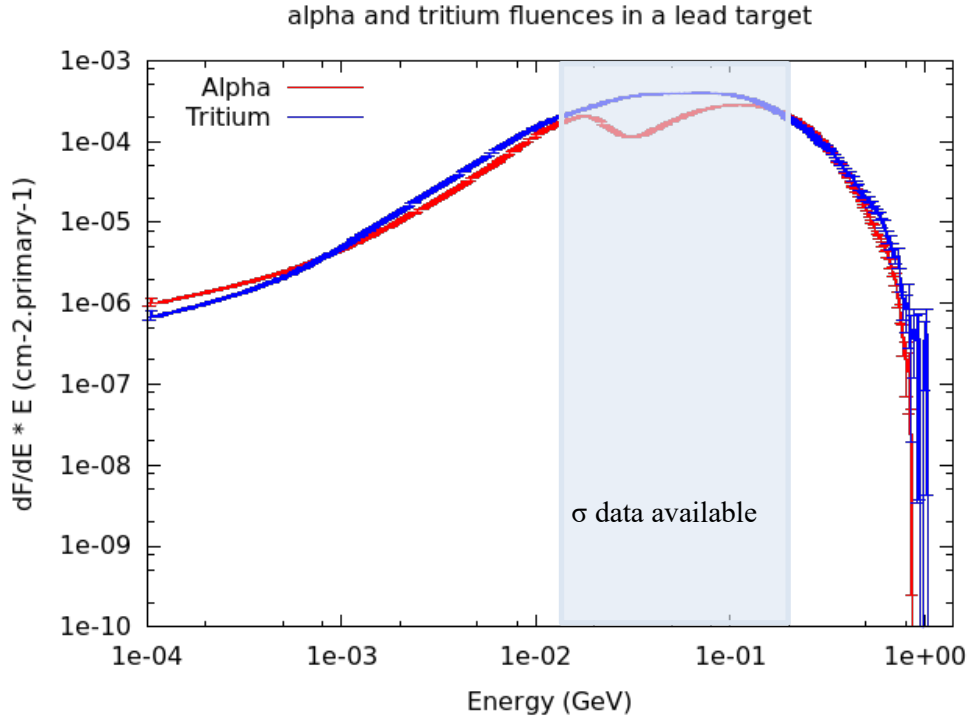


Fig. 3: ^3H and α particle fluence spectra (in lethargy) per primary in the lead target. The shape of the α fluence reflects the behaviour of the (p,α) reaction cross sections on the stable Pb isotopes.

The Hg-208 yield per primary can be calculated by solving the following equation:

$$\text{Yield.primary}^{-1} = \frac{N_A \cdot \rho}{A} V \int_{E_{\min}}^{E_{\max}} \frac{d\Phi}{dE} \sigma(E) dE \quad (1)$$

With N_A , the Avogadro number (in mol^{-1}), ρ the target density (in $\text{g}\cdot\text{cm}^{-3}$) (see Table 1), A the molar mass of the target material ($\text{g}\cdot\text{mol}^{-1}$), V the target volume (cm^3), Φ the fluence (in $\text{cm}^{-2}\cdot\text{primary}^{-1}$) and σ the cross section of the reaction of interest (in cm^2).

While cross-section data are commonly available as a point-wise continuous function of energy, the differential fluence obtained from Monte Carlo calculations is given in a discrete structure of n energy bins as $\frac{\Delta\Phi(E_i, E_{i+1})}{\Delta E}$ where $\Phi(E_i, E_{i+1})$ denotes the total fluence in the corresponding energy interval.

Therefore, the production cross-section data $\sigma(E)$ extracted from TENDL-2019, and shown in Figure 2, have been transformed into mean values given per discrete energy interval $\bar{\sigma}(E_i, E_{i+1})$, which correspond to the particle fluence's energy bins as given by FLUKA. As a consequence, the yield per primary has numerically been calculated as:

$$\text{Yield.primary}^{-1} = \frac{N_A \cdot \rho}{A} V \sum_{i=0}^{n-1} \frac{\Delta\Phi(E_i, E_{i+1})}{\Delta E} \bar{\sigma}(E_i, E_{i+1}) \Delta E \quad (2)$$

From this calculation, the Hg-208 yield is $1.5\text{E-}11$ nuclides per primary on Pb-208, with 92.5% of the production coming from the Pb-208($^3\text{H},3p$) reaction (see value in Table 1). However, when irradiating a Pb-nat target and considering that such target is composed of 52.4% Pb-208, one can expect to produce $7.8\text{E-}12$ Hg-208 atoms per primary on natural lead. The maximum relative uncertainty on this value is 0.7%. The uncertainty is only due to the statistical errors on the fluence spectra since no errors are given with the TENDL-2019 cross section values, which explains the low uncertainty on this value.

Figure 4 shows the distribution of the Hg yields in the lead target including the new yield value of $7.8\text{E-}12$ nuclides.primary⁻¹ extracted for Hg-208 on Pb-nat. The relative uncertainties on the production yields given by FLUKA RESNUCLEI are ranging from 0.3% (Hg-200) to 12.9% (Hg-207).

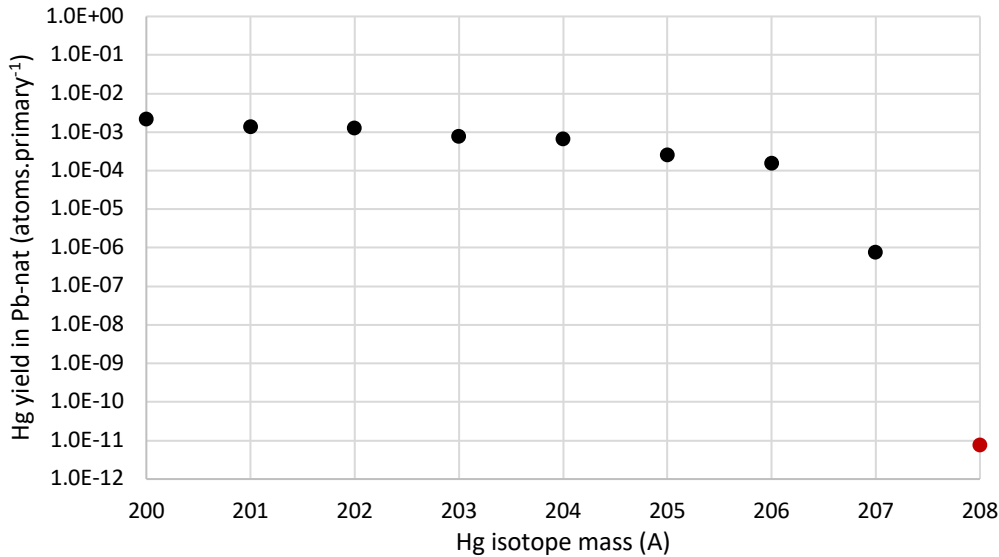


Fig. 4: Hg yields extracted from FLUKA (version 4.1) in a natural lead ISOLDE target between Hg-200 and Hg-207 (in black), with the addition of the Hg-208 yield value (in red) calculated in the present study.

However, one has to take into account that the production cross-section data for both reactions are available only up to 200 MeV. Our simulations shows that α particles can be produced in the lead target with an energy up to 840 MeV and the ^3H particles with an energy up to 1 GeV. Both cross-sections show a decreasing tendency at 200 MeV (see Figure 2). In order to compensate for the lack of data one can therefore consider as an upper estimate that the cross-sections will remain constant for both reactions from 200 MeV onwards. The cross-section value at 200 MeV is $3.1\text{E-}5$ mb for $\text{Pb-208}(^3\text{H},3\text{p})$ and $1.1\text{E-}5$ mb for $\text{Pb-208}(\alpha,4\text{p})$. Based on that assumption, an upper value of the Hg-208 yield in natural lead is obtained which is equal to $9.5\text{E-}12$, with 89% of the yield coming from the $\text{Pb-208}(^3\text{H},3\text{p})$ reaction. This shows that 82% of the total yield is already reached with ^3H and α particles with an energy up to 200 MeV.

3 Results

Table 1 summarizes the yields which have been calculated for twelve radionuclides produced by (α , xp) and (^3H , yp) reactions – with x ranging from 4 to 6 and y ranging from 3 to 5 - on lead, bismuth, thorium oxide and uranium carbide, by using the same methodology as the one presented in section 2. Column 3 and column 4 give the total α and ^3H fluences obtained in the target material presented in column 1 by considering the density given in column 2 and a target cylinder of 30.2 cm^3 irradiated by 1.4 GeV protons. The production yields presented in the last column are given for the corresponding nuclear reaction in column 6. One can see that the production of these radioisotopes is mainly dominated by the ^3H induced reactions. The contribution of the α reactions for such production is less than 10%. However, one should note that the values given in Table 1 have been calculated from the cross sections given by the TENDL-2019 library, which provides data only up to 200 MeV. Therefore, one should consider that these values are underestimating the experimental production yield that could be achieved for such isotopes.

Table 1: calculated yields (nuclei.primary⁻¹) in lead, bismuth, thorium and uranium thick ISOL targets

Target material	Density (g.cm ⁻³)	Total α fluence From 1E-4 to 1.4 GeV (cm ⁻² .primary ⁻¹)	Total ³ H fluence From 1E-4 to 1.4 GeV (cm ⁻² .primary ⁻¹)	Radionuclide of interest	Nuclear reactions	Q-value (MeV)	Calculated yield from TENDL cross section values (nuclei.primary ⁻¹)
Lead	10.7	7.61E-4 +/- 0.42%	1.14E-3 +/- 0.68%	Hg-208	Pb-208($\alpha,4p$)	-35.21	5.86E-13 +/- 0.44%
					Pb-208(³ H,3p)	-15.40	7.19E-12 +/- 0.73%
				Au-207	Pb-208($\alpha,5p$)	-45.00	1.92E-18 +/- 0.46%
					Pb-208(³ H,4p)	-25.10	1.01E-14 +/- 0.87%
				Pt-206	Pb-208($\alpha,6p$)	-53.40	1.41E-26 +/- 0.56%
					Pb-208(³ H,5p)	-33.60	6.12E-20 +/- 0.94%
Bismuth	9.8	7.78E-4 +/- 0.09%	1.15E-3 +/- 0.16%	Tl-209	Bi-209($\alpha,4p$)	-31.35	1.52E-12 +/- 0.09%
					Bi-209(³ H,3p)	-11.53	2.14E-11 +/- 0.16%
				Hg-208	Bi-209($\alpha,5p$)	-39.01	1.49E-17 +/- 0.09%
Bi-209(³ H,4p)	-19.20	4.09E-14 +/- 0.20%					
			Au-207	Bi-209($\alpha,6p$)	-48.80	6.82E-25 +/- 0.10%	
					Bi-209(³ H,5p)	-28.90	1.25E-18 +/- 0.23%
Thorium oxide	9.9	6.02E-4 +/- 0.48%	9.98E-4 +/- 0.72%	Ra-232	Th-232($\alpha,4p$)	-31.78	2.08E-12 +/- 0.52%
					Th-232(³ H,3p)	-11.97	3.48E-11 +/- 0.79%
				Fr-231	Th-232($\alpha,5p$)	-40.65	1.85E-18 +/- 0.55%
Th-232(³ H,4p)	-20.84	6.75E-14 +/- 0.95%					
			Rn-230	Th-232($\alpha,6p$)	-47.91	3.22E-22 +/- 0.65%	
					Th-232(³ H,5p)	-28.10	1.59E-19 +/- 1.03%
Uranium carbide	3.5	8.17E-4 +/- 0.66%	1.07E-3 +/- 1.05%	Th-238	U-238($\alpha,4p$)	-31.90	5.69E-13 +/- 0.66%
					U-238(³ H,3p)	-12.10	6.45E-12 +/- 1.28%
				Ac-237	U-238($\alpha,5p$)	-40.70	2.98E-19 +/- 0.69%
U-238(³ H,4p)	-20.90	1.51E-14 +/- 1.57%					
			Ra-236	U-238($\alpha,6p$)	-49.90	1.49E-26 +/- 0.79%	
					U-238(³ H,5p)	-30.08	1.24E-20 +/- 1.76%

4 Validation of the approach and with experimental data

These simulations were first validated by using data available from previous studies, notably with assessment of the production of the Bi-209($\alpha,2n$)At-211 reaction and by comparing the resulting yield with the one obtained from the FLUKA (version 4.1) predictions. The cross-section values of this reaction are high, reaching 1 barn at 30 MeV, which make easily possible the comparison with FLUKA. In this case, a bismuth target (cylinder radius = 0.7 cm, length = 19.6 cm, volume = 30.2 cm³, $\rho = 9.8$ g/cm³) irradiated with a 1.4 GeV proton beam has been considered. The α particle fluences have been retrieved together with the production cross section values from the FLUKA models and the yields given by FLUKA MC simulation. Both methods led to the same At-211 yield with a value of 3.9E-5 nuclei.primary⁻¹, which shows the consistency of the proposed approach with the FLUKA MC framework. When performing the same calculation with the TENDL-2019 library one gets a value of 3.3E-5 nuclei.primary⁻¹, which is due to the slight differences in the cross section data of 18%.

Additional verifications were performed on the ($\alpha,3p$) and (³H,2p) reactions on natural lead, bismuth, thorium and depleted uranium (see Table 2). However, large differences can be observed between the yield retrieved from the FLUKA MC simulations (using the RESNUCLEI card) and the calculated yield from TENDL-2019 cross-sections. When retrieving the cross sections used in FLUKA, one can find back the FLUKA yields obtained using the RESNUCLEI card and observe large differences between the cross sections estimated by FLUKA models (BME) and by TENDL-2019 (from TALYS) – see Figure 5. Therefore, one should note that the in-target production yields (Eq. (2)) presented in Table 1

and Table 2 are strongly dependent of the models and cross sections used. Please note that the TENDL cross sections are not given with any uncertainty which explains the low uncertainties reported in the last column of Table 2. However the FLUKA cross sections, generated by Monte Carlo, are provided with uncertainties which are directly related to the number of primaries that have been used (1E6 primaries in our case), which justifies the uncertainties given in the 4th column of Table 2. Table 2 shows that the discrepancies observed between FLUKA RESNUCLEI and the calculated yield from TENDL cross section are coming from a difference in the cross sections between FLUKA's models and TENDL-2019 (as clearly illustrated on Figure 5).

Table 2: simulated and calculated yields (nuclei.primary⁻¹) in lead, bismuth, thorium and uranium thick ISOL targets for ($\alpha,3p$) and ($^3\text{H},2p$) reactions

Target material	Radionuclide of interest	FLUKA Yield (nuclei.primary ⁻¹)	Calculated Yield from FLUKA cross sections (nuclei.primary ⁻¹)	Calculated Yield from TENDL cross sections (nuclei.primary ⁻¹)
Lead	Tl-209	1.9E-7 +/- 20.7%	2.2E-7 +/- 4.3%	1.4E-9 +/- 0.55%
Bismuth	Pb-210	6.4E-7 +/- 13.7%	6.0E-7 +/- 5.8%	4.1E-9 +/- 0.12%
Thorium	Ac-233	4.8E-7 +/- 18.1%	4.3E-7 +/- 5.7%	3.0E-9 +/- 0.61%
Uranium	Pa-239	1.3E-7 +/- 27.7%	1.5E-7 +/- 6.1%	7.9E-10 +/- 0.96%

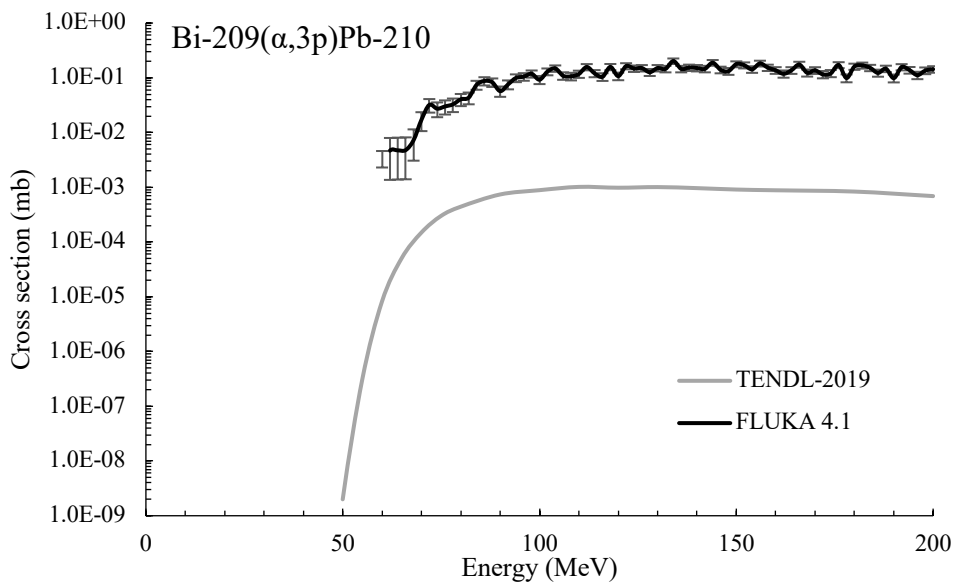


Fig. 5: example of discrepancies between FLUKA and TENDL-2019 cross sections on the reaction Bi-209($\alpha,3p$)Pb-210

Additional comparison was done with the assessment of the radionuclide inventory measured recently in LBE (lead bismuth eutectics) thick targets, notably to assess α and ^3H re-interaction with the thick target, through Bi-209($^3\text{H},3n$)At-209 and Bi-209($\alpha,4n$)At-209 [9].

Experimental rates of 5 to 25 pps (4.0E-12 nuclei.primary⁻¹ at 1 μA) have been detected for Hg-208 [1] after evaporation, diffusion, effusion, ionization, mass separation and transport to the experimental IDS station [10]. From our in-target production yield calculation using TENDL's cross section, one can expect to produce from 48 to 60 atoms of Hg-208 per μA (or 6.25E12 protons per second) during the irradiation of a natural lead target for one second, if the cross sections up to 200 MeV or over the full spectrum are considered. Release, diffusion and effusion can be estimated at 100% owing to the long half-life of this isotope as compared to the characteristic times of these different processes [11]. The ionization efficiency for Hg isotopes in VADIS ion sources [12] used with these molten lead targets has

been measured between 5 and 20%, and transport to the experimental stations of 70%, giving rates of between 2 to 10 pps, consistent with the experimental figures.

5 Impact of a 2 GeV proton beam energy on these reaction channels

Table 3 gives the comparison between the FLUKA yields obtained by MC simulations using a 1.4 GeV proton beam and a 2 GeV proton beam. One can see that in average an in-target production yield two times higher can be reached by increasing the PS Booster energy to 2 GeV and using the same ISOLDE target design has being currently used.

Table 3: comparison of the FLUKA yields (nuclei.primary⁻¹) between 1.4 GeV and 2 GeV in lead, bismuth, thorium and uranium thick ISOL targets for ($\alpha,3p$) and ($^3\text{H},2p$) reactions

Target material	Radionuclide of interest	FLUKA Yield at 1.4 GeV (nuclei.primary ⁻¹)	FLUKA Yield at 2 GeV (nuclei.primary ⁻¹)	Ratio 2 GeV/1.4 GeV
Lead	Tl-209	1.88E-7 +/- 20.7%	3.97E-7 +/- 20.6%	2.1
Bismuth	Pb-210	6.41E-7 +/- 13.7%	1.10E-6 +/- 9.5%	1.7
Thorium	Ac-233	4.75E-7 +/- 18.1%	7.53E-7 +/- 16.6%	1.6
Uranium	Pa-239	1.33E-7 +/- 27.7%	2.32E-7 +/- 28.0%	1.7

6 Conclusions

A computational method combining FLUKA with TENDL cross sections has been implemented to estimate the isotopes produced in thick targets from secondary particle re-interaction. Our method has been tested both with the production of At-211 which can be easily assessed with FLUKA due to the high values of its excitation function and with existing experimental data. These different comparisons provided a stringent test to show the consistency of our approach. We have applied this method for the production yield calculation of twelve isotopes induced by α and ^3H secondary reactions on lead, bismuth, thorium and uranium targets irradiated by 1.4 GeV protons at ISOLDE and MEDICIS [13]. New isotopes can thus be evaluated and become relevant for nuclidic inventories or for secondary beam production. However, significant differences have been observed between the cross sections used in FLUKA and the cross sections available in the TENDL-2019 library, for some isotopes evaluated here. New experimental measurement data would help in solving this issue.

7 References

[1] R. J. Carroll et al., Competition between allowed and first-forbidden β -decay: the case of $^{208}\text{Hg} \rightarrow ^{208}\text{Tl}$, Biophysical aspects of radiation quality, Phys Rev Letter. 2020 Nov 6; 125 (19): 192501. Doi: 10.1103/PhysRevLett.125.192501.

[2] C. Ahdida et al., "New Capabilities of the FLUKA Multi-Purpose Code", Frontiers in Physics 9, 788253 (2022). <https://doi.org/10.3389/fphy.2021.788253>

[3] G. Battistoni, T. Boehlen, F. Cerutti, P.W. Chin, L.S. Esposito, A. Fassò, A. Ferrari, A. Lechner, A. Empl, A. Mairani, A. Mereghetti, P. Garcia Ortega, J. Ranft, S. Roesler, P.R. Sala, V. Vlachoudis, G. Smirnov, Overview of the FLUKA code, Annals of Nuclear Energy 82, 10-18 (2015).

[4] FLUKA CERN Website <https://fluka.cern>

- [5] Tall Y., *et al.* *International Conference on Nuclear Data for Science and Technology*. EDP Sciences, 2007, p.1069, DOI: 10.1051/ndata:07762
- [6] T. Stora and R. S. Augusto, Production of ^{208}Hg at ISOLDE with a Pb target – a preliminary study, Dec 14, 2014. EDMS <https://edms.cern.ch/document/1866701/1>
- [7] Brunet, M., *et al.* "208Po populated through EC/ β^+ decay." *Journal of Physics: Conference Series*. Vol. 1643. No. 1. IOP Publishing, 2020. INPC2019 proceedings
- [8] A.J. Koning, D. Rochman, J. Sublet, N. Dzysiuk, M. Fleming and S. van der Marck, "TENDL: Complete Nuclear Data Library for Innovative Nuclear Science and Technology", Nuclear Data Sheets 155 (2019) 1. TENDL-2019 : TALYS-based evaluated nuclear data library available at https://tendl.web.psi.ch/tendl_2019/tendl2019.html
- [9] Choudhury, D, *Eur. Phys. J. A* **56**, 204 (2020). <https://doi.org/10.1140/epja/s10050-020-00191-z>
- [10] Fynbo H. *et al* (2017) *J. Phys. G: Nucl. Part. Phys.* 44 044005
- [11] Lettry J. *et al.* NIM B126 (1–4), 170 (1997).
- [12] Y. Martinez, PhD thesis, <http://cds.cern.ch/record/2672954/files/CERN-THESIS-2019-032.pdf>
- [13] Duchemin, C., *et al.* "CERN-MEDICIS: A review since commissioning in 2017." *Frontiers in Medicine* 8 (2021): 693682.